Chapter 19

Pumilio-based RNA in vivo imaging

Jens Tilsner*

Biomedical Sciences Research Complex, University of St Andrews, BMS Building, North Haugh, St Andrews, Fife KY16 9ST, United Kingdom

Cell & Molecular Sciences, The James Hutton Institute, Invergowrie, Dundee DD2 5DA, United Kingdom

*for correspondence

jt58@st-andrews.ac.uk

Running head: Pumilio-based RNA imaging

Summary

Subcellular, sequence-specific detection of RNA in vivo is a powerful tool to study the macromolecular transport that occurs through plasmodesmata. The RNA binding domain of Pumilio proteins can be engineered to bind RNA sequences of choice and fused to fluorescent proteins for RNA imaging. This chapter describes the construction of a Pumilio-based imaging system to track the RNA of *Tobacco mosaic virus* in vivo, and practical aspects of RNA live-cell imaging.

Key Words: RNA imaging, Pumilio homology domain, RNA binding protein, fluorescence complementation, protein engineering, fluorescent protein, fluorescence microscopy, *Tobacco mosaic virus*

1. Introduction

Plasmodesmata serve as intercellular conduits for different species of RNA between plant cells, including siRNAs mediating systemic posttranscriptional silencing *(1)*, miRNAs involved in developmental control *(2)*, the infectious genomes of RNA viruses and viroids *(3,4)*, and cellular mRNAs *(5,6)*. Therefore, techniques which permit the sequence-specific, dynamic localisation of RNAs in live cells are a valuable tool to study plasmodesmata function. A number of such techniques are now available (reviewed in *(7,8)*), but in walled plant cells, non-invasive, genetically encoded reporters are most easily applicable. Such systems use sequence-specific RNA binding proteins (RBPs) fused to fluorescent proteins (FPs), and are best suited to the detection of large RNA species such as viruses and mRNAs. Two classes of RBPs have been employed for generally applicable RNA imaging: bacteriophage-derived peptides that recognise the secondary structure of specific RNA stem-loops (see chapter by Peña in this volume), and the RNA-binding domain of Pumilio proteins.

Pumilio/FBF family (PUF) proteins are a group of sequence-specific RBPs that are ubiquitous in eukaryotes (26 genes in the *Arabidopsis* genome) and often function as translational repressors

(9-13). Their RNA-binding domain, the Pumilio homology domain (PUMHD) has a modular structure consisting of eight tandem repeats of a trihelical, 36 amino acid Puf motif. Each of these Puf repeats binds one nucleotide (Nt) in an eight-Nt binding motif that has no stable secondary structure. All contacts between the PUMHD and RNA are mediated by three amino acid side chains per Puf repeat, and the RNA bases. Amino acid side chains in positions 12 and 16 of each repeat form hydrogen bonds or van der Waals interactions with the Watson-Crick-edge of the RNA base whilst the side chain of amino acid 13 forms a stacking interaction *(14)*. Because only the interactions at position 12 and 16 are base-specific, the sequence-specificity of the PUMHD can be modified with just two amino acid modifications per repeat to bind to an RNA sequence of choice *(14-19)*.

To date, only the PUMHD of human Pumilio1 (HsPUM1-HD) has been used for RNA imaging, but in the future, PUMHDs derived from other PUF proteins may emerge as valuable alternatives and broaden the range of imaging possibilities. Pumilio-based RNA imaging has enabled subcellular detection of the mRNAs of mitochondrial NADH dehydrogenase and β-actin, as well as retroviral RNA in mammalian cultured cells *(20-23)*, and of the genomes of *Tobacco mosaic virus*, *Potato virus X* and *Turnip mosaic virus* in live plant tissue *(24-27)*. Of particular relevance to the topic of this volume, Pumilio-based RNA imaging has recently shown that *Potato virus X* is present in membrane structures at the entrances of plasmodesmata that also contain the viral replicase *(27)*.

The advantages of using modified PUMHDs for RNA imaging are 1) untagged, native RNA species expressed from their native genomic context can be localised *(20,21,24)*, avoiding both the need to modify the RNA and to introduce expression constructs into the genome; 2) if instead PUMHD recognition sequences are engineered into an RNA as a tag, no extensive secondary structures are introduced which might affect RNA function and localisation (though the PUMHD can actually access substantially structured target motifs *(18)*); 3) PUMHD variants can have 10- to 100-fold higher RNA affinities than stem-loop binding peptides used in alternative RNA imaging systems, thus PUMHD-based imaging is potentially more sensitive.

On the other hand, PUMHD RNA recognition has a degree of promiscuity *(28,29)*, and eukaryotic cells contain mRNA targets of native Pumilio proteins. Therefore, all Pumilio-based RNA imaging approaches use two PUMHD variants binding to the same target RNA to increase overall specificity and RNA affinity *(20,30)*. In the future, artificial PUMHDs with more than eight repeats that recognise longer target sequences may further improve the specificity of Pumilio-based RNA imaging *(18,30)*.

The adjustable sequence specificity of the PUMHD requires re-design and optimisation of Pumilio-based RNA imaging systems for any RNA of interest. Therefore, in the following paragraphs the considerations that have to be made when designing a PUMHD-based reporter system for a new RNA of interest are discussed, before providing a detailed protocol for imaging a specific RNA, that of *Tobacco mosaic virus* (TMV).

1.1. Choice of reporter system

When using any RBP-FP fusion for RNA imaging, it is necessary to distinguish between the RNA-bound and free states of the reporter, i.e. RNA-dependent signal and RNA-independent background. For PUMHD-based reporters, three different approaches have been used to identify RNA-bound fluorescence (**Fig. 1**). All systems use two PUMHD variants.

Nuclear targeting of a permanently fluorescent pair of fused PUMHDs (**Fig. 1A**) leads to confinement of fluorescence in the nucleus in the absence of target RNA. If the reporter is co-exported from the nucleus with a bound RNA, or binds to cytoplasmic RNA after translation, cytoplasmic fluorescence reveals the RNA's location. This approach is routinely used in RNA imaging with stem-loop binding bacteriophage peptides (see chapter by Peña in this volume). Attempts to apply the same principle to PUMHD-based imaging with two directly coupled PUMHDs fused to an FP and nuclear localisation signal (NLS) at their N-terminus (NLS-FP-PUMHD-PUMHD) proved unfeasible in plant cells because the reporter aggregated in the nucleus (unpublished data). However, a fusion with the FP inserted between the PUMHDs (NLS-PUMHD-FP-PUMHD) was recently used in mammalian cells *(23)* and may also work in plants.

Alternatively, the two PUMHD variants can be fused separately to two halves of a split FP, so that when both fusion proteins bind to the same target RNA, the split FP halves come into close proximity and re-fold into the complete FP, resulting in bimolecular fluorescence complementation (PUM-BiFC) at the location of the RNA *(20,24)* (**Fig 1B**). This principle is the only form of Pumilio-based RNA imaging so far applied in plants *(24-27)*.

Unfortunately, PUM-BiFC is not background-free. In BiFC, the fluorescent complex of N- and C-terminal split FP halves is extremely stable *(31)*. As the BiFC constructs accumulate in a cell, the increasing frequency of random collisions will result in the formation of low levels of reassembled FP, independent of interactions of fused PUMHDs with their cognate RNA. Additionally, due to their stability, PUM-BiFC complexes formed on the target RNA can dissociate from the RNA without 'switching off'. Both of these processes lead to the gradual accumulation of false-positive signal and thus reduce the signal-to-noise ratio. RNA-dependent PUM-BiFC signal has to be distinguished from this background by relative fluorescence levels and localisation (*see* **3.3.**). An additional side-effect of RNA-independent formation of PUM-BiFC complexes is that these pre-formed complexes can be recruited to the target RNA by the interaction of only one of the two PUMHDs. Thus, RNAs can be imaged with only a single binding site *(24,25)* or when the orientation of PUMHD fusions would be expected to prevent proximity of split FP halves after RNA binding (see below) *(22)*. Whilst this may sometimes be useful, it is not generally desirable, as it reduces the overall specificity of the PUM-BiFC system and eliminates the benefits of using two RNA binding domains.

Several recently developed approaches that improve the signal-to-noise ratio of BiFC by introducing further modifications into the split FP fragments *(31,32)* are still unexplored for PUM-BiFC applications. Also, a tetramolecular fluorescence complementation system for Pumilio-based RNA detection was recently introduced (PUM-TetFC) *(33)* (**Fig. 1C**) which has a very high signal-to-noise ratio in vitro, but is still untested in vivo. In PUM-TetFC, superfolder GFP is split into three fragments, the main β-barrel containing β-sheets 1-9, and the isolated β-

sheets 10 and 11, which are fused to the two PUMHD variants (the fourth component of TetFC is the RNA).

In the protocol following below, I describe the construction of a PUM-BiFC system as this is the only Pumilio-based approach so far used successfully in plants. However, as fluorescence complementation techniques are being continuously improved, it is recommended to consult relevant recent literature before constructing a novel PUM-BiFC system.

1.1.1. Choice of FP:

BiFC can be performed with various derivatives of both GFP and red FPs *(31,34-39)*. This allows selection of an FP that will facilitate co-localising the RNA of interest with other fluorescent markers that may already be available. In practice, only the GFP-derivatives EGFP, Venus and mCitrine have so far been used for PUM-BiFC, and of these, only PUMHD-split-mCitrine fusions in plants *(20,24)*. PUMHD fusions with split-mRFP1(Q66T) *(40)* failed to produce fluorescence in preliminary experiments (unpublished data).

1.1.2. Choice of FP splitting position:

Commonly, FPs are split either between β-sheets 7 and 8 (amino acids 154/155 or 157/158) or between β-sheets 8 and 9 (amino acids 172/173) *(31,34)*. Both have been employed in PUM-BiFC (EGFP, Venus split at 157/158 *(20)*, mCitrine split at 172/173 *(24)*). As it is the only PUM-BiFC system used in plants so far, fusions with mCitrine split between amino acids 172/173 are recommended until other split FPs have been tested.

1.1.3.Orientation of PUMHD-split FP fusions:

The PUMHD interacts with RNA in an antiparallel orientation, i.e. the N terminus is oriented towards the 3' and the C terminus towards the 5' end of the target sequence (**Fig. 2**). This means that the N terminus of the upstream and the C terminus of the downstream binding PUMHD will be in proximity to each other and have to be fused to the split FP halves. Fusing FP fragments at

the opposite ends (C terminus of upstream and N terminus of downstream PUMHD) prevents fluorescence complementation *(33)*. This leaves two possible choices of fusion orientations: if PUMHDs are fused to the N terminus of the FPN and the C terminus of the FPC fragment, they are attached to the natural termini of the FP. If PUMHDs are fused to the C terminus of FPN and the N terminus of FPC, they are attached to the rim of the FP β-barrel, with splitting positions between β-sheets 7 and 8 or 8 and 9 resulting in fusions to opposite rims of the β-barrel. Both configurations are possible and allow fluorescence complementation. Thus, the constraints imposed by the structures of both the PUMHD and the FP allow for two possible fusion combinations: FPC-PUMHD$_{upstream}$ + PUMHD$_{downstream}$-FPN, or FPN-PUMHD$_{upstream}$ + PUMHD$_{downstream}$-FPC. Only the latter combination has so far been used in RNA imaging and is therefore the recommended option *(20,21,24,33)*.

1.2. Choice of target sequences and PUMHD variants

PUM-BiFC imaging can be used in two different modes: PUMHDs can be modified to bind to the native RNA of interest *(20,21,23-25)*, or the RNA can be tagged with recognition motifs of previously characterised PUMHD variants *(22,24,26,27,33)* (**Table 1**). As described in the introduction, leaving the RNA unmodified has the advantage of avoiding potential RNA processing and localisation artefacts that could be caused by a tag, and by the expression of the tagged construct from an artificial genomic context. The latter is mainly a concern with nuclear mRNAs, not viruses. On the other hand, suitable binding sites that can be easily targeted with a limited number of PUMHD modifications may not be present in the RNA of interest, and whilst the binding specificity of modified PUMHDs can be predicted, it is harder to predict effects of modifications on RNA affinity, binding promiscuity, and protein solubility and stability *(15)*. Such potential problems can be avoided by using an RNA tag recognised by previously characterised PUMHD variants (**Table 1**), which can also increase specificity. For instance, Kellermann et al. *(33)* used a combination of wild-type PUMHD and Mut6-2/7-2 because these bind to their cognate targets with high affinities, but have low affinities for the binding sites of

the respective other variant *(15)*. The choice between modifying PUMHD variants or tagging the RNA will thus depend on considerations of the available target sequences and the suitability of previously characterised PUMHD variants for any given RNA.

Analyse the RNA of interest for the presence of sequences with similarity to native Pumilio binding sites. The target sequence of wild-type HsPUM1-HD is UGUANAUA (N = A, U, or C) *(29,41)* (**Fig. 2**) and most PUMHDs bind to sequences starting with a 5'UGU triplet *(29)*. This sequence motif is thus a good starting point for the identification of suitable target sequences. However, PUMHD variants with altered specificity of Puf repeats 6-8 (**Table 1**), which bind to the triplet, have also been used for RNA imaging and detection *(20,24,33)*. Plant RNA virus genomes often contain native Pumilio binding sites that can be exploited for PUM-BiFC imaging (and may be targets of native Pumilio proteins involved in host defense responses) *(24,25,42,43)*.

The two target sites should be closely adjacent, but separated by a short linker region to prevent steric hindrance of two simultaneously binding PUMHD fusions. With PUM-BiFC, dual target sites separated by linkers between 5 and 11 nucleotides long have been successfully imaged *(20-22,24)* (but *see* **Note 1**).

So far, modified PUMHD variants with up to five altered base specificities have been used for RNA imaging *(20,24)*, and with up to seven modified Puf repeats in engineered splicing factors *(19)*. However, with increasing numbers of amino acid changes, effects on overall RNA affinity and protein folding become more unpredictable.

If no suitable binding sites can be identified or very extensive PUMHD modifications would be required, and if no disadvantages from tagging the RNA are expected, select suitable previously described PUMHD variants, e.g. wild-type and mut6-2/7-2 PUMHD *(33)*, to design an RNA tag. In order to not disrupt open reading frames, RNA tags have to be inserted into untranslated regions. A good starting point is to introduce the tag directly downstream of an ORF immediately after the stop codon. Tagging upstream of the start codon may also work, and in some cases, several options may have to be tested *(24,44)*.

Table 1 lists previously characterised modified PUMHD variants ordered by alterations in their recognition sites from 5‘ to 3’, to facilitate easier selection of RNA target sites or tags. After selection of target sites or tags, the wild-type HsPUM1-HD needs to be modified into two different variants to bind the selected sequences. The molecular code for base-specificity of Puf repeats is as follows *(15,16,18,19,30,45)*:

$^{C}/_{S}$XXX**Q** = A

NXXX**Q** = U

SXXX**E** = G

$^{S}/_{T/G/C/A}$XXX**R** = C

where the letters represent amino acids 12-16 of each Puf repeat, and X in positions 13-15 are amino acids not involved in base specificity. In the HsPUM1 ORF, the relevant amino acids corresponding to residues 12 and 16 in each repeat, respectively, are: Puf1 [863, 867]; Puf2 [899, 903]; Puf3 [935, 939]; Puf4 [*971*, 975]; Puf5 [1007, 1011]; Puf6 [1043, 1047]; Puf7 [1079, 1083]; Puf8 [1122, 1126] (**Table 1**). The italicised residue 971 in Puf4 does not actually participate in RNA interactions *(14,15)*). The amino acids in position 13, which contribute stacking interactions to RNA binding, are left unchanged (*see* **Note 2**). Avoid using Puf4/Nt5 modifications as a main specificity determinant (*see* **Note 3**).

1.3. Choice of expression system

In principle, PUM-BiFC reporter constructs can be stably expressed, but so far all Pumilio-based RNA imaging in plants has been done with transient expression systems (agroinfiltration or microprojectile bombardment) *(24-27)*. Since nonspecific background fluorescence increases with the accumulation of the PUM-BiFC fusions, transient expression may be preferable as it permits limiting background fluorescence by reducing the expression time (*see* **3.3.**). Agroinfiltration is generally preferable to biolistic bombardment, as it leads to reporter expression in large tissue areas, and makes it easier to assess cell-to-cell variability of PUM-BiFC signal and find optimal imaging conditions (*see* **3.3.**). It is therefore recommended to use

agroinfiltration as the first choice of expression system. However, when viral RNAs are imaged, co-expression of agrobacterium-delivered plasmids and virus can be problematic and in that case, bombardment provides a useful alternative means of delivering reporter constructs.

After these general considerations, the following protocol describes the construction of a PUM-BiFC system to image the untagged, genomic RNA of *Tobacco mosaic virus* (TMV) *(24,26)*.

2. Materials

1. A plasmid containing a *HsPUM1-HD* ORF (encoding amino acids Gly828-Gly1176 of the full-length HsPUM1 protein) as a PCR template (available from www.openbiosystems.com).
2. A plasmid containing a *Citrine* fluorescent protein ORF as a PCR template, e.g. pSAT6-Citrine-N1 (GeneBank acc. AY818369) *(46)*.
3. Primers (*see* **Table 2**).
4. Standard molecular cloning materials: Commercial kits for high-fidelity PCR amplification, PCR clean up, DNA gel extraction, and plasmid minipreps; PCR machine; gel chamber and power supply for running horizontal agarose gels; benchtop centrifuges; electrocompetent *E.coli* cells, e.g. strain DH5α, and electroporator; LB media (liquid and agar plates) containing either 50 μg/ml gentamicin or 100 μg/ml spectinomycin; 37°C shaking and non-shaking incubators.
5. Gateway™ vectors pDONR207 (LifeTechnologies) and pGWB402Ω *(47)*.
6. Gateway™ BP and LR Clonase (LifeTechnologies).
7. Electrocompetent *Agrobacterium tumefaciens* cells, strain AGL1; LB media (liquid and agar plates) containing either 100 μg/ml spectinomycin and 50 μg/ml rifampicin; 28°C shaking and non-shaking incubators.
8. Infiltration medium:10 mM MES pH 5.6, 10 mM $MgCl_2$, 15 μM acetosyringone.
9. Spectrophotometer for measuring optical density at 600 nm (OD_{600}).

10. Gauge 25 needles.
11. 1 ml syringes.
12. 3-4 weeks old *Nicotiana benthamiana* plants.
13. An infectious clone of TMV which must contain nucleotides 3794-3816 (within the 183k RNA polymerase domain), e.g. TMV.DsRed *(24)*.
14. A commercial kit for RNA in vitro transcription with an RNA polymerase matching the infectious TMV construct (T7 for TMV.DsRed).
15. Aluminium oxide powder.
16. A confocal laser-scanning microscope equipped with 514 and 561 nm excitation light sources and suitable detection systems for mCitrine and mRFP. An upright microscope equipped with water-dipping lenses is the preferable setup for imaging intact plant tissue in vivo.

3. Methods

3.1. Modification of PUMHDs

To direct one PUMHD variant (PUMHD3794) to bind to the sequence UGUAGAUA (nucleotides 3794-3801 of the TMV genome), the specificity of Puf4 needs to be modified (U5G: N971S/H972N/Q975E). A second PUMHD variant (PUMHD3809) is engineered to bind the sequence UGAUAGUU (nucleotides 3809-3816 of TMV) by altering the specificities of Puf1 (A8U: S863N), 3 (A6G: C935S/Q939E), 4 (U5A: N971C), 5 (A4U: C1007N), and 6 (U3A: N1043C).

1. PUMHD3794 (*see* **Fig. 3A** for schematic of the construction process and finished fusion construct):

   PCR#1:Amplify an N-terminal fragment of PUMHD3794 from a wild-type PUMHD template using primer pair link-PUMfor/U5G_441rev (see **Table 1** for all primer sequences used in this protocol. All primers are designed for annealing at 55°C). Use a proof-reading, high fidelity polymerase according to manufacturer's instructions, but amplify for only 10 cycles to minimize the likelihood of PCR errors. The link-PUMfor

primer adds the flexible GGGGS linker that will connect the PUMHD to the N-terminal mCitrine fragment (see below) and a unique *Xba*I site for easy exchange of PUMHD variants.

2. Gel-purify the ~0.4 kb PCR product on a 2% agarose gel using a commercial gel extraction kit. The PCR product will serve as the template in the next PCR reaction and gel purification removes the wild-type PUMHD template that would otherwise be amplified in the next PCR.
3. PCR#2: Amplify the purified N-terminal PUMHD fragment again, this time with primers link-PUMfor/U5G_449rev and again using only 10 PCR cycles.
4. PCR#3: From the wild-type PUMHD template, amplify a ~0.6 kb C-terminal fragment of PUMHD3794 using primers U5G_434for/attB-PUMrev (10 cycles only). Gel-purify the product as above. The attB-PUMrev primer adds a Gateway attB2 anchor as well as a unique *Xho*I site for easy exchange of PUMHD variants.
5. PCR#4: Amplify the C-terminal fragment again using primers U5G_425for/attB-PUMrev (10 cycles).
6. PCR#5 (overlap PCR of full-length PUMHD3794): The four U5G primers have introduced all three required point mutations and also created a 25 bp overlap between the N- and C-terminal fragments. Using the products of PCR#2 and #4 as templates, amplify the ~1.05 kb full-length PUMHD3794 using primers link-PUMfor/attB-PUMrev with 10 PCR cycles.
7. PUMHD3809 (*see* **Fig. 3B**):

   The multiple mutations introduced in this PUMHD variant require a multi-step overlap PCR. As above, use a high-fidelity polymerase and only 10 PCR cycles for each PUMHD fragment. All PCR products amplified from wild-type template need to be gel-purified before proceeding to subsequent overlap PCR steps.

8. PCR#1: Amplify an N-terminal 0.12 kb fragment of PUMHD3809 using primers attB-PUMfor/A8U_119rev. Gel-purify. The attB-PUMfor primer adds a Gateway attB1 anchor, as well as a unique *Xba*I site for easy exchange of PUMHD variants.
9. PCR#2: Amplify a ~0.2 kb fragment from bp 95-333 of PUMHD3809 using primers A8U_095for/A6G_333rev1. Gel-purify.
10. PCR#3: Extend PCR#2 product by amplification with primers A8U_095for/A6G_333rev2.
11. PCR#4: Amplify a 0.12 kb fragment from bp 323-440 of PUMHD3809 using primers A6G_323for/U5A_440rev. Gel-purify.
12. PCR#5: Amplify a 0.32 kb overlap-product from bp 95-440 of PUMHD3809 using both PCR#3 and PCR#4 products as templates and primers A8U_095for/U5A_440rev.
13. PCR#6: Amplify a 0.44 kb overlap product from bp 1-440 of PUMHD3809 using both PCR#1 and PCR#5 products as templates, and primers attB-PUMfor/U5A_440rev.
14. PCR#7: Amplify a ~0.13 kb fragment from bp 416-549 of PUMHD3809 using primers U5A_416for/A4U_549rev. Gel-purify.
15. PCR#8: Amplify a 0.55 kb overlap product from bp 1-549 of PUMHD3809 using both PCR#6 and PCR#7 products as templates, and primers attB-PUMfor/A4U_549rev.
16. PCR#9: Amplify a ~0.13 kb fragment from bp 527-658 of PUMHD3809 using primers A4U_527for/U3A_658rev. Gel-purify.
17. PCR#10: Amplify a 0.66 kb overlap product from bp 1-658 of PUMHD3809 using both PCR#8 and PCR#9 products as templates, and primers attB-PUMfor/U3A_658rev.
18. PCR#11: Amplify a ~0.43 kb C-terminal fragment of PUMHD3809 using primers U3A_625for/link-PUMrev. Gel-purify. The link-PUMrev primer extends the PUMHD with the flexible GGGGS linker that will connect it to the C-terminal fragment of mCitrine (see below) and also adds a unique *Xho*I site for easy exchange of PUMHD variants.
19. PCR#12 (overlap PCR of full-length PUMHD3809): Amplify ~1.05 kb full-length PUMHD3809 using both PCR#10 and PCR#11 products as templates, and primers attB-PUMfor/link-PUMrev.

3.2. Construction of PUMHD-split mCitrine fusions

1. Amplify the 0.52 kb N-terminal fragment of Citrine fluorescent protein (CitN; amino acids 1-172) using a plasmid encoding Citrine (e.g. pSAT-Citrine-N1 *(46)*) as the template, and primers attB-Citfor/link-CitNrev (high-fidelity polymerase, 10 PCR cycles). The attB-Citfor primers adds a Gateway attB1 anchor, while the link-CitNrev primer adds the GGGGS linker for connection to PUMHD3794.
2. Amplify a C-terminal fragment of Citrine (mCitC; amino acids 173-239) in an overlap PCR that introduces the A206K mutation which prevents dimerization of GFP and its derivatives *(48,49)*: Amplify two ~0.1 kb fragments in separate PCRs using primers link-CitCfor/Citmonorev and Citmonofor/attB-Citrev, respectively, from a Citrine-encoding plasmid (high-fidelity polymerase, 10 cycles). The link-CitCfor primer adds the GGGGS linker that will connect to PUMHD3809. The attB-Citrev primer adds a Gateway attB2 anchor. After gel-purification, amplify the complete C-terminal fragment of monomerized Citrine (mCitC) using both partial PCR products as templates, and primers link-CitCfor/attB-Citrev (10 cycles).
3. Amplify the complete CitN-PUMHD3794 fusion using CitN and full-length PUMHD3794 PCR products as templates, and primers attB1-adapter/attB2-adapter. Use a high-fidelity polymerase and 20 PCR cycles. Run a 5 μl aliquot of the PCR reaction on a 1% agarose gel. If there is a single, 1.6 kb product, remove remnants of the PCR reaction using a commercial PCR clean up kit. If more than one PCR product was obtained, run the rest of the PCR out on the gel, and excise and gel-purify the 1.6 kb band using a commercial kit.
4. Amplify the complete PUMHD3809-mCitC fusion using full-length PUMHD3809 and mCitC PCR products as templates, and primers attB1-adapter/attB2-adapter. Use a high-fidelity polymerase and 20 PCR cycles. Run a 5 μl aliquot of the PCR reaction on a 1% agarose gel. If there is a single, 1.3 kb product, remove remnants of the PCR reaction using a commercial PCR clean up kit. If more than one PCR product was obtained, run the

rest of the PCR out on the gel, and excise and gel-purify the 1.3 kb band using a commercial kit.

5. Recombine both CitN-PUMHD3795 and PUMHD3809-mCitC products into a Gateway DONR vector, e.g. pDONR207 (Gent^R), using Gateway™ BP recombinase (LifeTechnologies) according to manufacturer's instructions. Transform the BP recombination into *E.coli* competent cells and plate on LB agar containing 50 μg/ml gentamicin. On the next day, pick several colonies for overnight culture in LB liquid media containing gentamicin, then isolate the plasmids using a commercial kit. Verify that the mCitN-PUMHD3794 and PUMHD3809-CitC fusions have no PCR errors by sequencing the DONR vector inserts.
6. Recombine error-free fusion constructs into a Gateway destination binary vector for plant expression, e.g. pGWB402Ω (Spec^R; *(46)*), using Gateway™ LR Clonase (LifeTechnologies) according to manufacturer's instructions. Transform the LR reaction into *E. coli* competent cells and plate on LB agar containing 100 μg/ml spectinomycin. On the next day, pick several colonies for overnight culture in LB liquid media containing spectinomycin, then isolate the plasmids using a commercial kit. Check that correct expression constructs were obtained by diagnostic restriction digest (e.g. excising the ~1.05 kb PUMHD using *Xba*I/*Xho*I).

3.3. PUM-BiFC in vivo imaging

1. Transform CitN-PUMHD3794 and PUMHD3809-mCitC binary expression vectors separately into electrocompetent *Agrobacterium tumefaciens* cells strain AGL1 (other strains are also suitable). Plate the transformed agrobacteria on LB agar containing 100 μg/ml spectinomycin to select for transformants, and 50 μg/ml rifampicin to suppress growth of other bacteria. Grow plates at 28°C for two days.
2. Transcribe TMV.DsRed *(24)* RNA in vitro, using a commercial T7 polymerase kit according to manufacturer's instructions. Keep the RNA on ice after transcription. Infect 3-4 weeks old *Nicotiana benthamiana* plants by dusting the leaves thinly with aluminium

oxide power and then gently rub-inoculating 5-10 μl transcript with a gloved hand (*see* **Note 4**). Incubate plants at 33°C after infection.

3. Two days after infection, pick single colonies into 4 ml liquid LB media containing spectinomycin and rifampicin and grow in a shaking incubator at 28°C for two days (*see* **Note 5**).
4. Pellet the bacterial cultures, then resuspend each pellet into 2 ml infiltration medium.
5. Incubate the resuspended agrobacteria at room temperature in the dark for about 1 h, then measure the OD_{600}.
6. Mix and dilute CitN-PUMHD3794 and PUMHD3809-mCitC-containing agrobacteria with infiltration medium so that both are present at OD_{600} = 0.25 in the final mixture (i.e. total combined OD_{600} = 0.5).
7. With the tip of a needle, create small incisions on the abaxial (lower) side of uninfected and TMV-infected *Nicotiana benthamina* leaves by gently touching the leaf surface with the needle so that a dark point is just visible.
8. Carefully infiltrate the agrobacterium mixture into these incisions using a 1 ml syringe without a needle pressed on the incision site (*see* **Note 6**). Ca. 1-2 ml of suspension are required to cover a leaf. Agrobacteria can be infiltrated in patches, e.g. overlapping with virus-infected issue areas, or into the entire leaf lamina, depending on experimental requirements.
9. For imaging, place whole or half leaves or ~2 x 2 cm leaf pieces under a microscope lens by fixing them to a microscope slide using double-sided sticky tape, with the lower epidermis facing up. An upright microscope with water-dipping lenses, which can be directly immersed in a drop of water placed on the leaf with no cover glass in between, is ideal for plant imaging. Excite mCitrine BiFC at 514 nm and detect mCitrine fluorescence at 520-550 nm. Excite DsRed at 561 nm and detect DsRed fluorescence at 570-600 nm.
10. Begin imaging by monitoring the level and localisation of background fluorescence in uninfected tissue every day from 1-4 days post infiltration (dpi). (*See* **Note 7**). Expect

false-positive BiFC fluorescence to be distributed fairly homogenously throughout the nucleoplasm and cytoplasm. The nucleus tends to be brighter than the cytoplasm. At very high expression levels or in small cells, PUM-BiFC may aggregate.

11. In parallel to uninfected control plants, image the PUM-BiFC reporter constructs in TMV-infected tissue, also daily from 1-4 dpi (corresponding to 5-8 days after TMV infection). Compared to the negative control, expect increased fluorescence intensity (*see* **Note 8**), and also a re-localisation. In particular, nucleoplasmic signal usually disappears in the presence of target RNA and instead of general cytoplasmic fluorescence, the PUM-BiFC signal is expected to be concentrated in granular viral replication sites which can be small and dispersed in the cytoplasm, or aggregated into a large perinuclear inclusion body (*24,25*) (**Fig. 4**).
12. Monitoring BiFC for several days after infiltration and comparing the signal intensity and localization in uninfected and infected tissue establishes a suitable time window for obtaining a good signal-to-noise ratio (*see* **Note 9**). Once this has been accomplished, the time span separating infection and reporter infiltration can be varied (*see* **step 3** above) to follow the TMV RNA localisation throughout the infection cycle (*see* **Note 10**).

4. Notes

1. Kellermann et al. *(33)* found that a 7 nucleotides long linker between PUMHD binding sites was optimal for PUM-TetFC, and de- or increasing it to 5 or 9 nucleotides, respectively, significantly reduced the fluorescent signal. The length of a suitable linker will depend on the length and flexibility of the protein linker between PUMHD and FP fragment, but it should be kept in mind that the greater tolerance of PUM-BiFC for different linker lengths may actually be due to recruitment of pre-formed PUM-BiFC complexes to the RNA by just one of the two PUMHDs (*see* **1.1.**). In PUM-BiFC systems with improved signal-to-noise ratio, linker length may become more critical and may have to be empirically optimised.

2. Amino acid residues that participate in stacking interactions with the RNA bases can also contribute to base specificity, and their modification can either increase or decrease binding promiscuity *(19,50)*. However, modifying these residues can also negatively affect overall RNA affinity and protein solubility *(15,50)*. Therefore, until a systematic investigation has led to a detailed understanding of stacking interactions in HsPUM1-HD, it is recommended that amino acids at position 13 of the Puf repeats are not modified.
3. Note that Puf4 in the wild-type PUMHD can promiscuously bind any base at position 5 *(29)*. Puf4 differs slightly from the other Puf repeats in that its Asn971 in position 12 does not contact the RNA base, whereas Gln975 can interact either with the Watson-Crick edge of U, the Hoogsteen edge of A or G, or not contact the base at all when a C is in position 5. Whilst binding specificity of Puf4 can be modified, the fifth base of target sequences should therefore not be used as a critical specificity determinant, e.g. as the only difference between two target sites.

   Position 8, bound by Puf1 also shows some promiscuity and can accept G instead of A *(15)*, whilst other promiscuous binding modes of Puf3 and 7 have lower affinities for non-cognate bases but these may still be in a range that permits binding during RNA imaging in vivo *(15,20)*. Lastly HsPUM1-HD can bind 9 nucleotide sequences by flipping one base out away from the protein surface *(28)*. It is useful to be aware of these alternative binding modes when choosing target sites for imaging and creating modified PUMHD variants.
4. The infectious TMV clone does not have to express a fluorescent protein, but this helps to identify infected leaf areas. Encapsidating transcribed RNA into TMV capsid protein in vitro, passaging TMV from infectious lesions, or expressing the TMV genome in planta from a CaMV 35S promoter (e.g. pTRBO; *(51)*) following either DNA rub-inoculation, microprojectile bombardment, or agroinfiltration are also suitable methods of infection.
5. It is useful to make glycerol stocks of transformed agrobacteria to save time when repeatedly growing liquid cultures for imaging.

6. Young leaves are easier to infiltrate as they have larger airspaces. Avoid pressing the opening on the syringe too hard onto the leaf surface as this will cause extensive damage. Also, if air spaces in the mesophyll are tight causing a high resistance to the infiltration, increasing the injection pressure is more likely to cause agrobacterium mixture to squirt out sideways from under the rim of the syringe than to improve infiltration.
7. Since folding and stability of split FP fragments are influenced by fusion partners such as the PUMHD variants (which may themselves differ in their respective in vivo folding efficiency and stability), unfused split FP halves are no suitable negative control in BiFC. Ideal BiFC controls are fusions with non-interacting variants of the proteins used in the actual experiments (*31*). In the case of PUM-BiFC this corresponds to either the absence of the target RNA as described here, or PUMHD fusions that do not bind the target RNA *(24,33)*. Background fluorescence due to random collisions should be the same for both types of controls. However, the ability to bind cellular RNAs promiscuously, as well as the folding efficiency and stability of the PUMHD-split FP fusions may differ for different pairs of PUMHDs. Therefore, expressing the target RNA-specific reporter constructs in the absence of the target provides the best negative control.
8. Make sure not to oversaturate images during acquisition. Differences in fluorescence intensity between infected cells and uninfected controls are only apparent when images are not overexposed. Try to work at the lowest possible gain settings to maximise the contrast.
9. A direct comparison between nonspecific and TMV-dependent BiFC levels may be difficult because viruses often suppress other ectopic expression constructs to a considerable degree. It may be necessary to increase OD_{600} and expression time for infected tissue compared with the negative control.
10. PUM-BiFC expression levels may need to be re-optimised when imaging different infection stages. In strongly infected tissue at late infection stages, expression of the RNA reporter constructs may be too strongly suppressed to produce sufficient PUM-BiFC

signal for imaging. Conversely at early infection stages, if PUM-BiFC accumulates too much compared to viral RNA levels, the signal-to-noise ratio will be too low to clearly localise the viral RNA over the background.

To compensate for such effects, PUMHD fusion constructs can be agroinfiltrated at an OD_{600} between ~0.1 and 1.0 each (at a 1:1 ratio). It may also be worth experimenting with unequal expression ratios to optimise the signal-to-noise ratio and minimize aggregation *(24)*.

Even after optimisation of imaging conditions, expression levels are usually very heterogenous throughout the tissue and across viral lesions. The number of cells that have an optimal virus/PUM-BiFC ratio at a specific viral infection stage may be very small in a single experiment. It is therefore important to observe large areas of tissue and repeat experiments to both find suitable imaging conditions and ensure their reproducibility.

5. References

1. Dunoyer P., Schott G., Himber C. et al. (2010) Small RNA duplexes function as mobile silencing signals between plant cells. *Science* **328**, 912-916
2. Carlsbecker A., Lee J.Y., Roberts C.J. et al. (2010) Cell signalling by microRNA165/6 directs gene dose-dependent root cell fate. *Nature* **465**, 316-321
3. Wang Y., Ding B. (2010) Viroids: small probes for exploring the vast universe of RNA trafficking in plants. *J Integr Plant Biol* **52**, 28-39
4. Niehl A., Heinlein M. (2011) Cellular pathways for viral transport through plasmodesmata. *Protoplasma* **248**, 75-99
5. Lucas W.J., Bouché-Pillon S., Jackson D.P. et al. (1995) Selective trafficking of KNOTTED1 homeodomain protein and its mRNA through plasmodesmata. *Science* **270**, 1980-1983

6. Kim J.Y., Rim Y., Wang J. et al. (2005) A novel cell-to-cell trafficking assay indicates that the KNOX homeodomain is necessary and sufficient for intercellular protein and mRNA trafficking. *Genes Dev* **19**, 788-793
7. Tyagi S. (2009) Imaging intracellular RNA distribution and dynamics in living cells. *Nat Meth* **6**, 331-338
8. Christensen N.M., Oparka K.J., Tilsner J. (2010) Advances in imaging RNA in plants. *Trends Plant Sci* **15**, 196-203
9. Wickens M., Bernstein D.S., Kimble J. et al. (2002) A PUF family portrait: 3'UTR regulation as a way of life. *Trends Genet* **18**, 150-157
10. Francischini C.W., Quaggio R.B. (2009) Molecular characterization of *Arabidopsis thaliana* PUF proteins - binding specificity and target candidates. *FEBS J* **276**, 5456-5470
11. Tam P., Barrette-Ng I., Simon D. et al. (2010) The Puf family of RNA-binding proteins in plants: phylogeny, structural modeling, activity and subcellular localization. *BMC Plant Biol* **10**, 44
12. Abbasi N., Park Y.I., Choi S.B. (2011) Pumilio Puf domain RNA-binding proteins in Arabidopsis. *Plant Signal Behav* **6**, 364-368
13. Quenault T., Lithgow T., Traven A. (2011) PUF proteins: repression, activation and mRNA localization. *Trends Cell Biol* **21**, 104-112
14. Wang X., McLachlan J., Zamore P.D. et al. (2002) Modular recognition of RNA by a human Pumilio-homology domain. *Cell* **110**, 501-512
15. Cheong C.G., Tanaka Hall T.M. (2006) Engineering RNA sequence specificity of Pumilio repeats. *Proc Natl Acad Sci USA* **103**, 13635-13639
16. Lu G., Dolgner S.J., Tanaka Hall T.M. (2009) Understanding and engineering RNA sequence specificity of PUF proteins. *Curr Op Struct Biol* **19**, 110-115
17. Mackay J.P., Font J., Segal D.J. (2011) The prospects for designer single-stranded RNA-binding proteins. *Nat Struct Mol Biol* **18**, 256-261

18. Filipovska A., Razif M.F.M., Nygård K.K.A. et al. (2011) A universal code for RNA recognition by PUF proteins. *Nat Chem Biol* **7**, 425-427
19. Dong S., Wang Y., Cassidy-Amstutz C. et al. (2011) Specific and modular binding code for cytosine recognition in Pumilio/FBF (PUF) RNA-binding domains. *J Biol Chem* **286**, 26732-26742
20. Ozawa T., Natori Y., Sato M. et al. (2007) Imaging dynamics of endogenous mitochondrial RNA in single living cells. *Nat Meth* **4**, 413-419
21. Yamada T., Yoshimura H., Inaguma A. et al. (2011) Visualization of nonengineered single mRNAs in living cells using genetically encoded fluorescent probes. *Anal Chem* **83**, 5708-5714
22. Yu S.F., Lujan P., Jackson D.L. et al. (2011) The DEAD-box RNA helicase DDX6 is required for efficient encapsidation of a retroviral genome. *PLoS Pathog* **7**, e1002303
23. Yoshimura H., Inaguma A., Yamada T. et al. (2012) Fluorescent probes for imaging endogenous β-actin mRNA in living cells using fluorescent protein-tagged Pumilio. *ACS Chem Biol* **7**, 999-1005
24. Tilsner J., Linnik O., Christensen N.M. et al. (2009) Live-cell imaging of viral RNA genomes using a Pumilio-based reporter. *Plant J* **57**, 758-770
25. Wei T., Huang T.S., McNeil J. et al. (2010) Sequential recruitment of the endoplasmic reticulum and chloroplasts for plant potyvirus replication. *J Virol* **84**, 799-809
26. Tilsner J., Linnik O., Wright K.M. et al. (2012) The TGB1 movement protein of potato virus X re-organises actin and endomembranes into the 'X-body' a viral replication factory. *Plant Physiol* **158**, 1359-1370
27. Tilsner J., Linnik O., Louveaux M. et al. (2013) Replication and trafficking of a plant virus are coupled at the entrances of plasmodesmata. *J Cell Biol* **201**, 981-995
28. Gupta Y.K., Nair D.T., Wharton R.P. et al. (2008) Structures of human Pumilio with noncognate RNAs reveal molecular mechanisms for binding promiscuity. *Structure* **16**, 549-557

29. Lu G., Tanaka Hall T.M. (2011) Alternate modes of cognate RNA recognition by human PUMILIO proteins. *Structure* **19**, 361-367
30. Wang Y., Wang Z., Tanaka Hall T.M. (2013) Engineered proteins with Pumilio/fem-3 mRNA binding factor scaffold to manipulate RNA metabolism. *FEBS J*. doi:10.1111/febs.12367
31. Kodama Y., Hu C.-D. (2012) Bimolecular fluorescence complementation (BiFC): A 5-year update and future perspectives. *BioTechniques* **53**, 285-298
32. Li M., Doll J., Weckermann K. et al. (2010) Detection of in vivo interactions between Arabidopsis class A-HSFs, using a novel BiFC fragment, and identification of novel class B-HSF interacting proteins. *Europ J Cell Biol* **89**, 126-132
33. Kellermann S.J., Rath A.K., Rentmeister A. (2013) Tetramolecular fluorescence complementation for detection of specific RNAs in vitro. *ChemBioChem* **14**, 200-204
34. Hu C.D., Kerppola T.K. (2003) Simultaneous visualization of multiple protein interactions in living cells using multicolor fluorescence complementation analysis. *Nat Biotechnol* **21**, 539-545
35. Lee L.Y., Fang M.J., Kuang L.Y. et al. (2008) Vectors for multi-color bimolecular fluorescence complementation to investigate protein-protein interactions in living plant cells. *Plant Methods* **4**, 24
36. Waadt R., Schmidt L.K., Lohse M. et al. (2008) Multicolor bimolecular fluorescence complementation reveals simultaneous formation of alternative CBL/CIPK complexes in planta. *Plant J* **56**, 505-516
37. Gehl C., Waadt R., Kudla J. et al. (2009) New GATEWAY vectors for high throughput analyses of protein-protein interactions by bimolecular fluorescence complementation. *Mol Plant* **2**, 1051-1058
38. Qin L., Chu J., Zheng Y. et al. (2009) A new red bimolecular fluorescence complementation based on TagRFP. *Proc SPIE* **7191**, 71910G

39. Zilian E., Maiss E. (2011) An optimized mRFP-based bimolecular fluorescence complementation system for the detection of protein-protein interactions in planta. *J Virol Meth* **174**, 158-165
40. Jach G., Pesch M., Richter K. et al. (2006) An improved mRFP1 adds red to bimolecular fluorescence complementation. *Nat Meth* **3**, 597-600
41. Morris A.R., Mukherjee N., Keene J.D. (2008) Ribonomic analysis of human Pum1 reveals cis-trans conservation across species despite evolution of diverse mRNA target Sets. *Mol Cell Biol* **28**, 4093-4103
42. Huh S.U., Kim M.J., Paek K.H. (2013) Arabidopsis Pumilio protein APUM5 suppresses Cucumber mosaic virus infection via direct binding of viral RNAs. *Proc Natl Acad Sci USA* **110**, 779-784
43. Huh S.U., Paek K.H. (2013) Role of Arabidopsis Pumilio RNA binding protein 5 in virus infection. *Plant Signal Behav* **8**, e23975
44. Lange S., Katayama Y., Schmid M. et al. (2008) Simultaneous transport of different localized mRNA species revealed by live-cell imaging. *Traffic* **9**, 1256-1267
45. Filipovska A., Rackham O. (2011) Designer RNA-binding proteins: new tools for manipulating the transcriptome. *RNA Biol* **8**, 978-983
46. Tzfira T., Tian G.-W., Lacroix B. et al. (2005) pSAT vectors: a modular series of plasmids for autofluorescent protein tagging and expression of multiple genes in plants. *Plant Mol Biol* **57**, 503-516
47. Nakagawa T., Suzuki T., Murata S. et al. (2007) Improved Gateway binary vectors: high-performance vectors for creation of fusion constructs in transgenic analysis of plants. *Biosci Biotechnol Biochem* **71**, 2095-2100
48. Zacharias D.A., Violin J.D., Newton A.C. et al. (2002) Partitioning of lipid-modified monomeric GFPs into membrane microdomains of live cells. *Science* **296**, 913-916
49. Shaner N.C., Steinbach P.A., Tsien R.Y. (2005) A guide to choosing fluorescent proteins. *Nat Meth* **2**, 905-909

50. Koh Y.Y., Wang Y., Qiu C. et al. (2011) Stacking interactions in PUF-RNA complexes. *RNA* **17**, 718-727
51. Lindbo J.A. (2007) TRBO: A high-efficiency Tobacco mosaic virus RNA-based overexpression vector. *Plant Physiol* **145**, 1232-1240
52. Wang Y., Cheong C.G., Tanaka Hall T.M. et al. (2009) Engineering splicing factors with designed specificities. *Nat Meth* **6**, 825-830

Figure Captions

Figure 1. Methods to distinguish RNA-bound and unbound PUMHD reporters. A. Relocalisation of a nuclear-targeted, permanently fluorescent double-PUMHD fusion to the cytoplasm in the presence of target RNA *(23)*. B. Assembly of a bimolecular fluorescence complementation complex on the target RNA (PUM-BiFC) *(20)*. This is the approach described in this protocol. C. Assembly of a tetramolecular fluorescence complementation complex on the target RNA (PUM-TetFC) *(33)*.

Figure 2. Base-specific interactions between the HsPUM1-HD and its target sequence. Dotted lines represent hydrogen bonds and parentheses represent van der Waals contacts. Modified from *(14,15)*.

Figure 3. Construction schematics and finished PUMDH-split mCitrine fusions for TMV imaging. A. CitN-PUMHD3794. B. PUMHD3809-mCitC.

Figure 4. Example of TMV RNA imaged with the PUM-BiFC system. Viral RNA is visible in small punctae dispersed throughout the cytoplasm and a large perinuclear inclusion body (arrow). N: nucleus. Scale bar: 50 μm.

Table Captions

Table 1. RNA-contacting amino acid residues and cognate targets of HsPUM1-HD variants. For each variant, Puf repeats from Puf8 to Puf1 (C- to N-terminal direction) and RNA sequences in 5'-3' orientation are shown from left to right in each row; amino acid residues 16, 13, and 12 are shown from top to bottom in each column. PUMHD variants are listed in order of changes to the target sequence specificity in 5' to 3' direction. Changes in amino acids and RNA targets are highlighted in bold and shaded. Italicised N971 does not contribute to RNA contacts in HsPUM1-HD. Where absolute dissociation constants have been determined for the shown target sequence, these are listed (n.d.: not determined). Note that dissociation constants for promiscuously bound alternate target sequences are not shown. These are always higher than for the main target, but may well be in a range suitable for RNA imaging purposes (refer to original publications for alternative k_D's and relative binding activities of individual PUMHD variants, in particular *(15)*).

Table 2. Primers required for construction of a PUM-BiFC system to image untagged TMV RNA in vivo. *Xba*I and *Xho*I restriction sites are underlined, mutagenic nucleotides highlighted by boldface font and shading.

Table 1: Modified HsPUM1-HD variants

PUMHD	**Puf8**	**Puf7**	**Puf6**	**Puf5**	**Puf4**	**Puf3**	**Puf2**	**Puf1**	**References**
wild-type	Q1126	E1083	Q1047	Q1011	Q975	Q939	Q903	Q867	*(14,22,24,25,33,53)*
	Y1123	N1080	Y1044	R1008	H972	R936	Y900	R864	
	N1122	S1079	N1043	C1007	*N971*	C935	N899	S863	
k_D = 0.5 nM	U	G	U	A	U/C	A	U	A	
U1C	**R1126**	E1083	Q1047	Q1011	Q975	Q939	Q903	Q867	*(18)*
	Y1123	N1080	Y1044	R1008	H972	R936	Y900	R864	
	G1122	S1079	N1043	C1007	*N971*	C935	N899	S863	
k_D n.d.	**C**	G	U	A	U/C	A	U	A	

PUF#2	**R1126**	**Q1083**	**E1047**	Q1011	Q975	Q939	**R903**	Q867	*(19)*
	Y1123	N1080	Y1044	R1008	H972	R936	Y900	R864	
	S1122	**N1079**	**S1043**	C1007	*N971*	C935	**S899**	S863	
k_D n.d.	**C**	**U**	**G**	A	U/C	A	**C**	A	
PUF-E	**E1126**	**R1083**	Q1047	**E1011**	Q975	Q939	**E903**	**R867**	*(19)*
	Y1123	**Y1080**	Y1044	R1008	H972	R936	Y900	**Y864**	
	S1122	S1079	N1043	**S1007**	*N971*	**N935**	**S899**	S863	
k_D n.d.	**G**	**C**	U	**G**	U/C	**U**	**G**	**C**	
PUF#1	**E1126**	**R1083**	**E1047**	**E1011**	Q975	**E939**	Q903	**E867**	*(19)*
	Y1123	**Y1080**	Y1044	R1008	H972	R936	Y900	R864	
	S1122	S1079	**S1043**	**S1007**	*N971*	**S935**	**C/S 899**	S863	
k_D n.d.	**G**	**C**	**G**	**G**	U/C	**G**	**A**	**G**	
Mut7-2	Q1126	**Q1083**	Q1047	Q1011	Q975	Q939	Q903	Q867	*(15)*
	Y1123	N1080	Y1044	R1008	H972	R936	Y900	R864	
	N1122	**N1079**	N1043	C1007	*N971*	C935	N899	S863	
k_D = 6.0 nM	U	**U**	U	A	U/C	A	U	A	
R7($S^N/_Y$xxR)	Q1126	**R1083**	Q1047	Q1011	Q975	Q939	Q903	Q867	*(19)*
	Y1123	N/**Y** 1080	Y1044	R1008	H972	R936	Y900	R864	
	N1122	S1079	N1043	C1007	*N971*	C935	N899	S863	
k_D n.d.	U	**C**	U	A	U/C	A	U	A	
G2C	Q1126	**R1083**	Q1047	Q1011	Q975	Q939	Q903	Q867	*(18)*
	Y1123	N1080	Y1044	R1008	H972	R936	Y900	R864	
	N1122	**G1079**	N1043	C1007	*N971*	C935	N899	S863	

k_D n.d.	U	**C**	U	A	U/C	A	U	A	
Mut6-2/7-2 =	Q1126	**Q1083**	**E1047**	Q1011	Q975	Q939	Q903	Q867	*(15,33,53)*
Var1	Y1123	N1080	Y1044	R1008	H972	R936	Y900	R864	
	N1122	**N1079**	**S1043**	C1007	*N971*	C935	N899	S863	
k_D = 18 nM	U	**U**	**G**	A	U/C	A	U	A	
Mut7-2/3-1	Q1126	**Q1083**	Q1047	Q1011	Q975	Q939	Q903	Q867	*(15)*
	Y1123	N1080	Y1044	R1008	H972	R936	Y900	R864	
	N1122	**N1079**	N1043	C1007	*N971*	**N935**	N899	S863	
k_D = 0.6 nM	U	**U**	U	A	U/C	**U**	U	A	
U3A	Q1126	E1083	Q1047	Q1011	Q975	Q939	Q903	Q867	*(18)*
	Y1123	N1080	Y1044	R1008	H972	R936	Y900	R864	
	N1122	S1079	**C1043**	C1007	*N971*	C935	N899	S863	
k_D n.d.	U	G	**A**	A	U/C	A	U	A	
U3G	Q1126	E1083	**E1047**	Q1011	Q975	Q939	Q903	Q867	*(18)*
	Y1123	N1080	Y1044	R1008	H972	R936	Y900	R864	
	N1122	S1079	**S1043**	C1007	*N971*	C935	N899	S863	
k_D n.d.	U	G	**G**	A	U/C	A	U	A	
mPum2	Q1126	E1083	**E1047**	Q1011	Q975	Q939	Q903	Q867	*(14,20)*
	Y1123	N1080	**N1044**	R1008	H972	R936	Y900	R864	
	N1122	S1079	**S1043**	C1007	*N971*	C935	N899	S863	
k_D = 92 nM	U	G	**G**	A	U/C	A	U	A	
R6($S^Y/_H$xxR)	Q1126	E1083	**R1047**	Q1011	Q975	Q939	Q903	Q867	*(19)*
	Y1123	N1080	Y/**H** 1044	R1008	H972	R936	Y900	R864	

	N1122	S1079	**S1043**	C1007	*N971*	C935	N899	S863	
k_D n.d.	U	G	**C**	A	U/C	A	U	A	
U3C	Q1126	E1083	**R1047**	Q1011	Q975	Q939	Q903	Q867	*(18)*
	Y1123	N1080	Y1044	R1008	H972	R936	Y900	R864	
	N1122	S1079	**G/A/S/ T/C 1043**	C1007	*N971*	C935	N899	S863	
k_D n.d.	U	G	**C**	A	U/C	A	U	A	
PUF-B	Q1126	E1083	**R1047**	Q1011	Q975	Q939	Q903	**E867**	*(19)*
	Y1123	N1080	Y1044	R1008	H972	R936	Y900	R864	
	N1122	S1079	**S1043**	**N1007**	*N971*	C935	N899	S863	
k_D n.d.	U	G	**C**	**U**	U/C	A	U	**G**	
PUF-C	Q1126	E1083	**R1047**	Q1011	Q975	**R939**	Q903	**E867**	*(19)*
	Y1123	N1080	Y1044	R1008	H972	**Y936**	Y900	R864	
	N1122	S1079	**S1043**	**N1007**	*N971*	**S935**	N899	S863	
k_D n.d.	U	G	**C**	**U**	U/C	**C**	U	**G**	
mPum1	Q1126	E1083	Q1047	Q1011	**S975**	**E939**	Q903	Q867	*(20)*
	Y1123	N1080	**N1044**	R1008	H972	R936	Y900	R864	
	N1122	S1079	**C1043**	**N1007**	*N971*	**S935**	N899	**N863**	
k_D = 163 nM	U	G	**A**	**U**	**G**	**G**	U	**U**	
T3809	Q1126	E1083	Q1047	Q1011	Q975	**E939**	Q903	Q867	*(24,26,27)*
	Y1123	N1080	Y1044	R1008	H972	R936	Y900	R864	
	N1122	S1079	**C1043**	**N1007**	**C971**	**S935**	N899	**N863**	
k_D n.d.	U	G	**A**	**U**	**A**	**G**	U	**U**	
PUF-D	Q1126	E1083	**R1047**	Q1011	**E975**	**R939**	Q903	**E867**	*(19)*

	Y1123	N1080	Y1044	R1008	**Y972**	**Y936**	Y900	R864	
	N1122	S1079	**S1043**	**N1007**	**S971**	**S935**	N899	S863	
k_D n.d.	U	G	**C**	**U**	**G**	**C**	U	**G**	
R6/R2(SYxxR)	Q1126	E1083	**R1047**	Q1011	Q975	Q939	**R903**	Q867	*(19)*
	Y1123	N1080	Y1044	R1008	H972	R936	Y900	R864	
	N1122	S1079	**S1043**	C1007	*N971*	C935	**S899**	S863	
	U	G	**C**	A	U/C	A	**C**	A	
PUF-A	Q1126	E1083	**R1047**	Q1011	Q975	Q939	Q903	**E867**	*(19)*
	Y1123	N1080	Y1044	R1008	H972	R936	Y900	R864	
	N1122	S1079	**S1043**	C1007	*N971*	C935	N899	S863	
k_D n.d.	U	G	**C**	A	U/C	A	U	**G**	
R5($S^R/_Y$xxR)	Q1126	E1083	Q1047	**R1011**	Q975	Q939	Q903	Q867	*(19)*
	Y1123	N1080	Y1044	R/**Y** 1008	H972	R936	Y900	R864	
	N1122	S1079	N1043	**S1007**	*N971*	C935	N899	S863	
k_D n.d.	U	G	U	**C**	U/C	A	U	A	
A4C	Q1126	E1083	Q1047	**R1011**	Q975	Q939	Q903	Q867	*(18)*
	Y1123	N1080	Y1044	R1008	H972	R936	Y900	R864	
	N1122	S1079	N1043	**G1007**	*N971*	C935	N899	S863	
k_D n.d.	U	G	U	**C**	U/C	A	U	A	
actPUM2	Q1126	E1083	Q1047	**E1011**	Q975	Q939	**E903**	Q867	*(23)*
	Y1123	N1080	Y1044	R1008	H972	R936	Y900	R864	
	N1122	S1079	C1043	**S1007**	*N971*	**N935**	**S899**	**N863**	
k_D n.d.	U	G	U	**G**	U/C	**U**	**G**	**U**	

mPUM4	Q1126	E1083	Q1047	**E1011**	Q975	**E939**	**E903**	Q867	*(21)*
	Y1123	N1080	Y1044	R1008	H972	R936	Y900	R864	
	N1122	S1079	C1043	**S1007**	*N971*	**N935**	**S899**	**N863**	
k_D n.d.	U	G	U	**G**	U/C	**U**	**G**	**U**	
T3794	Q1126	E1083	Q1047	Q1011	**E975**	Q939	Q903	Q867	*(22,24,26,27)*
	Y1123	N1080	Y1044	R1008	**N972**	R936	Y900	R864	
	N1122	S1079	N1043	C1007	**S971**	C935	N899	S863	
k_D n.d.	U	G	U	A	**G**	A	U	A	
U5C	Q1126	E1083	Q1047	Q1011	**R975**	Q939	Q903	Q867	*(18)*
	Y1123	N1080	Y1044	R1008	H972	R936	Y900	R864	
	N1122	S1079	N1043	C1007	**G971**	C935	N899	S863	
k_D n.d.	U	G	U	A	**C**	A	U	A	
Mut3-1	Q1126	E1083	Q1047	Q1011	Q975	Q939	Q903	Q867	*(15)*
	Y1123	N1080	Y1044	R1008	H972	R936	Y900	R864	
	N1122	S1079	N1043	C1007	*N971*	**N935**	N899	S863	
k_D = 0.5 nM	U	G	U	A	U/C	**U**	U	A	
Mut3-2 = mPUM3	Q1126	E1083	Q1047	Q1011	Q975	**E939**	Q903	Q867	*(15,21,53)*
	Y1123	N1080	Y1044	R1008	H972	R936	Y900	R864	
	N1122	S1079	N1043	C1007	*N971*	**S935**	N899	S863	
k_D = 0.05 nM	U	G	U	A	U/C	**G**	U	A	
A6C	Q1126	E1083	Q1047	Q1011	Q975	**R939**	Q903	Q867	*(18)*
	Y1123	N1080	Y1044	R1008	H972	R936	Y900	R864	
	N1122	S1079	N1043	C1007	*N971*	**G935**	N899	S863	
k_D n.d.	U	G	U	A	U/C	**C**	U	A	

R3(SYxxR)-Y972	Q1126	E1083	Q1047	Q1011	Q975	**R939**	Q903	Q867	*(19)*
	Y1123	N1080	Y1044	R1008	**Y972**	R/**Y**936	Y900	R864	
	N1122	S1079	N1043	C1007	*N971*	**S935**	N899	S863	
k_D n.d.	U	G	U	A	U/C	**C**	U	A	
actPUM1	Q1126	E1083	Q1047	Q1011	Q975	**E939**	Q903	**E867**	*(23)*
	Y1123	N1080	Y1044	R1008	H972	R936	Y900	R864	
	N1122	S1079	N1043	C1007	*N971*	**S935**	N899	S863	
k_D n.d.	U	G	U	A	U/C	**G**	U	**G**	
R2(SYxxR)	Q1126	E1083	Q1047	Q1011	Q975	Q939	**R903**	Q867	*(19)*
	Y1123	N1080	Y1044	R1008	H972	R936	Y900	R864	
	N1122	S1079	N1043	C1007	*N971*	C935	**S899**	S863	
k_D n.d.	U	G	U	A	U/C	A	**C**	A	
U7C	Q1126	E1083	Q1047	Q1011	Q975	Q939	**R903**	Q867	*(18)*
	Y1123	N1080	Y1044	R1008	H972	R936	Y900	R864	
	N1122	S1079	N1043	C1007	*N971*	C935	**G899**	S863	
k_D n.d.	U	G	U	A	U/C	A	**C**	A	
Mut1-1	Q1126	E1083	Q1047	Q1011	Q975	Q939	Q903	**E867**	*(15)*
	Y1123	N1080	Y1044	R1008	H972	R936	Y900	R864	
	N1122	S1079	N1043	C1007	*N971*	C935	N899	S863	
k_D = 1.3 nM	U	G	U	A	U/C	A	U	**G**	
A8C	Q1126	E1083	Q1047	Q1011	Q975	Q939	Q903	**R867**	*(18)*
	Y1123	N1080	Y1044	R1008	H972	R936	Y900	R864	
	N1122	S1079	N1043	C1007	*N971*	C935	N899	**G863**	
k_D n.d.	U	G	U	A	U/C	A	U	**C**	

Table 2: Oligonucleotide primers for constructing a PUM-BiFC system to image TMV RNA

Primer name	Sequence (5'→3')
attB-PUMfor	AAAAAGCAGGCTCTAGATGGGCAGGAGCAGGCTTTTGG
attB-PUMrev	AGAAAGCTGGGTCTCGAGTTATCCCTAAGTCAACACCGTTCTTCATG
link-PUMfor	GGAGGTGGTGGATCTAGAGGCAGGAGCAGGCTTTTGG
link-PUMrev	AGATCCACCACCTCCCTCGAGTCCCTAAGTCAACACCGTTCTTCATG
A8U_095for	ACCAGCATGGG**AA**CAGATTCATTCAG
A8U_119rev	TGAATGAATCTG**TT**CCCATGCTGGTC
A6G_323for	GCCGTGTTATC**G**AGAAAGCTCTTGAG
A6G_333rev1	GATAACACGGC**T**GCCATACATCTGTAG
A6G_333rev2	TCAAGAGCTTTCT**C**GATAACACGGC**T**GCCATACATCTGTAG
U5G_425for	ATGGCA**G**T**A**ACGTGGTT**G**AGAAATG
U5G_434for	ACGTGGTT**G**AGAAATGCATTGAATGTG
U5G_441rev	AACCACGT**T**A**C**TGCCATTCTGATCTTTCAC
U5G_449rev	CATTTCT**C**AACCACGT**T**A**C**TGCCATTCTGATCTT
U5A_416for	AAGATCAGAATGGC**TG**TCACGTGGTTC
U5A_440rev	ACCACGTGA**CA**GCCATTCTGATCTTTC
A4U_527for	ATCCTTATGGC**AA**CCGAGTGATTCAG
A4U_549rev	AATCACTCGG**TT**GCCATAAGGATGTG
U3A_625for	CTTGTACAGGATCAATATGGA**TG**TTATGTAATCC
U3A_658rev	GGATTACATAA**CA**TCCATATTGATCCTGTACAAG
attB-Citfor	AAAAAGCAGGCTATGGTGAGCAAGGGCGAGG
attB-Citrev	AGAAAGCTGGGTTTACTTGTACAGCTCGTCCATGCCG
link-CitNrev	TCTAGATCCACCACCTCCGTCCTCGATGTTGTGGCGGATC
link-CitCfor	CTCGAGGGAGGTGGTGGATCTGGCAGCGTGCAGCTCGC
Citmonofor	CTACCAGTCC**AAA**CTGAGCAAAGAC
Citmonorev	GTCTTTGCTCAG**TTT**GGACTGGTAG

attB1-adapter	GGGGACAAGTTTGTACAAAAAAGCAGGCT
attB2-adapter	GGGGACCACTTTGTACAAGAAAGCTGGGT

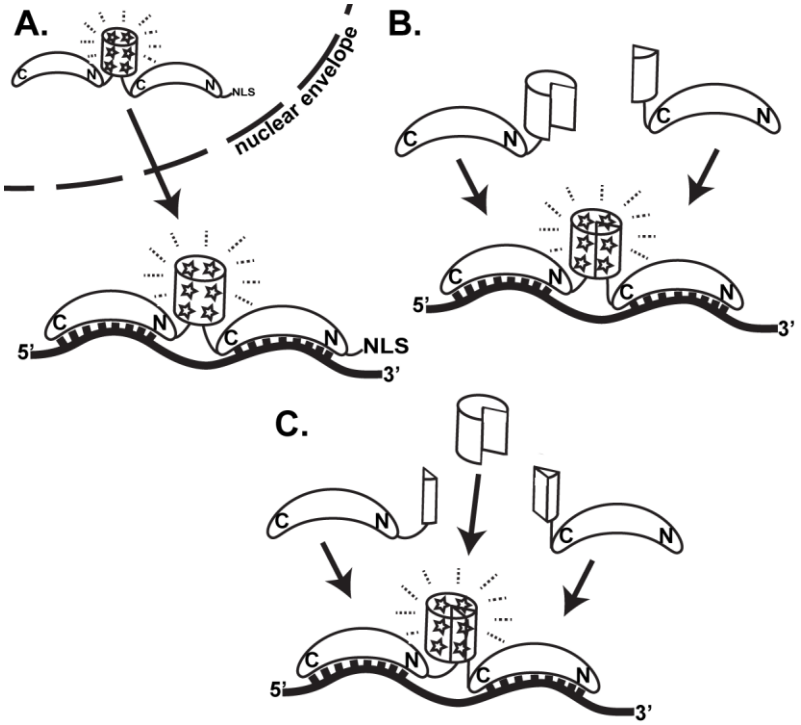

Figure 1

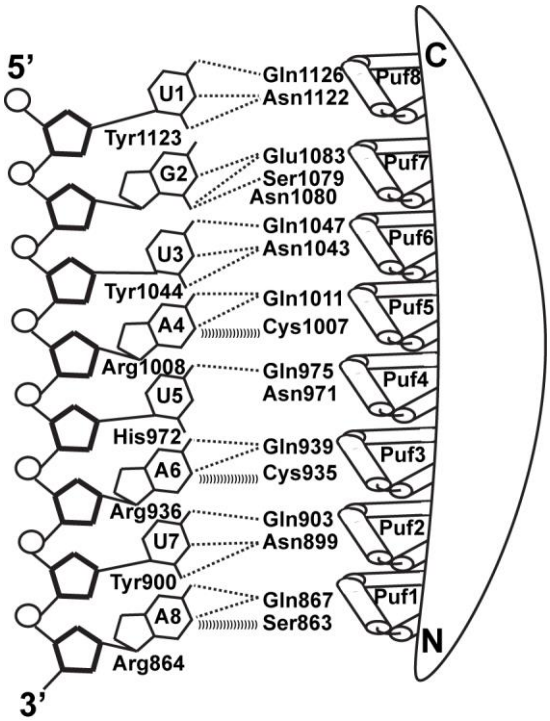

Figure 2

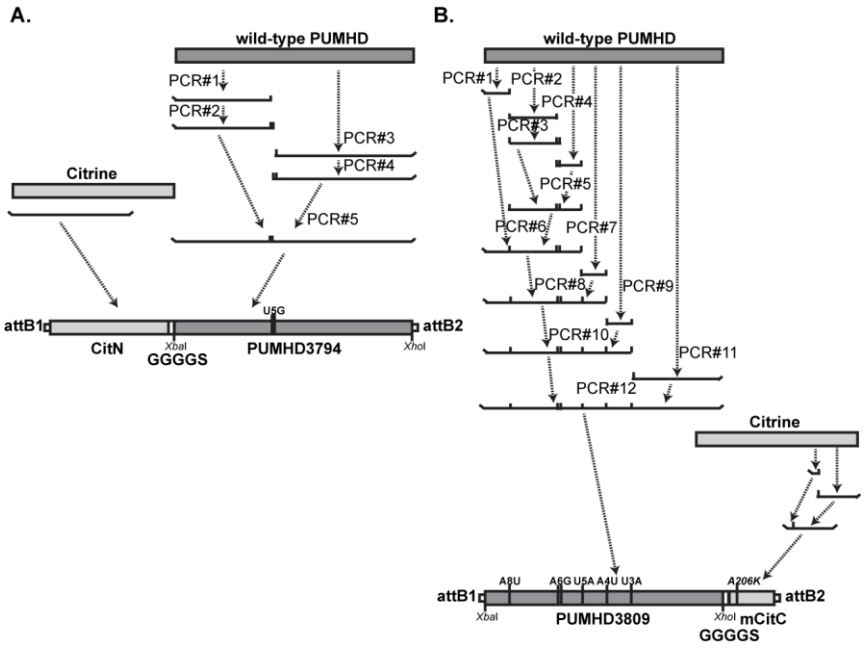

Figure 3

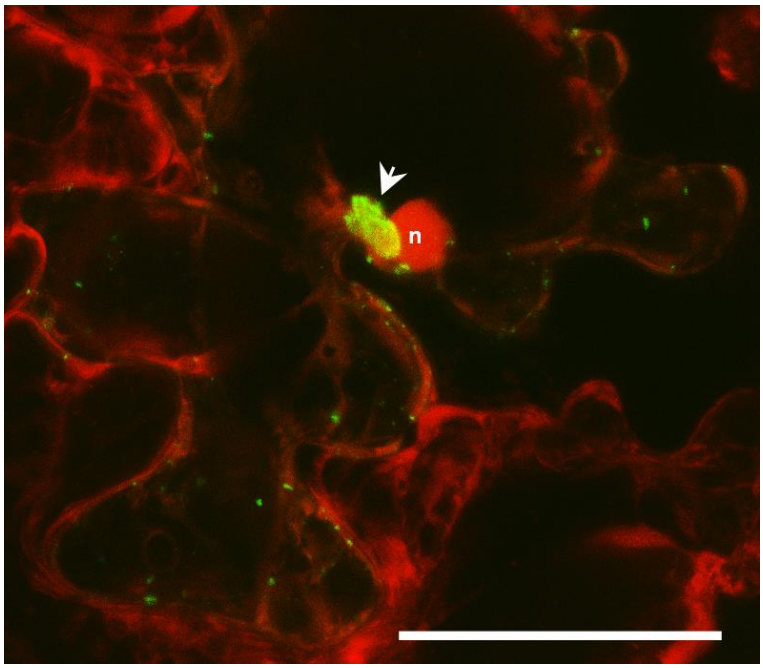

Figure 4